Contaminant intrusion in water distribution systems

SAHEB MANSOUR-REZAEI,[1] GHOLAMREZA NASER,[1] AHMAD MALEKPOUR,[2] AND BRYAN W. KARNEY[2]

[1]Okanagan School of Engineering, University of British Columbia, Kelowna, B.C.
[2]Department of Civil Engineering, University of Toronto, Toronto, Ont.

The research described in this article concerns contaminant intrusion into a water distribution system associated with transient events. A Lagrangian-based contaminant transport model was coupled with an Eulerian-based transient hydraulic model to study contaminant intrusion and its propagation in a water distribution system. The hydraulic model was used to detect negative pressures during normal system operations. The Lagrangian-based contaminant transport model reduced simulation time and avoided numerical dissipation and dispersion errors that often occur with Eulerian-based modeling. The proposed water quality model was used to evaluate two systems described in the literature for their potential vulnerability to contaminant intrusion. The new transient water quality model realistically simulated intrusion events and contaminant propagation in both systems.

Keywords: *contaminant intrusion, Eulerian model, Lagrangian model, transient pressure, water distribution systems, water quality modeling*

Disturbances in water quality can occur anywhere along a water supply system from the water source(s) to the treatment plant and from transmission mains to consumers. Although water utilities monitor water quality for some contaminants at sources and treatment plants (NRCC, 2004) and take necessary action if required, outbreaks of endemic disease sometimes occur as a result of the intrusion of contaminants into distribution systems.

Payment et al (1997) reported an excess of credible gastrointestinal illnesses in 14–40% of drinking water consumers in Canada. Schuster et al (2005) reported 288 disease outbreaks resulting from contaminated Canadian water distribution systems between 1974 and 2001. At least 8,000 cases of illness were linked to these outbreaks, but the real number could be 10 to 1,000 times higher, depending on the severity of symptoms (Environment Canada, 2001). Borchardt et al (2009) found viruses in water samples collected from household taps, and Besner et al (2011) reported that these viruses had likely entered the distribution system. The 1993 outbreak of waterborne disease in Milwaukee, Wis., resulted in at least 104 deaths, more than 400,000 cases of illness, and an estimated cost of $96.2 million (Corso et al, 2003). These outbreaks—along with those in Walkerton, Ont., in 2000 (seven deaths, 2,300 illnesses, and a cost of $64.5 million) and North Battleford, Sask., in 2001 (40–50% of residents became sick)—suggest that the consequences of a waterborne disease outbreak could be catastrophic.

Water quality failures are likely to occur more frequently as a result of the continued deterioration of aging distribution systems and the effects of climate change, urbanization, and emerging contaminants on water resources. Regardless of how, where, or why a contaminant entered a distribution system, an oversimplified model can delay or entirely miss the detection of hydraulic or water quality failures by providing inaccurate or misleading estimates of flow parameters. Such inaccuracies could result in economic loss, human illness, or death.

In 2005 AWWA highlighted metal accumulation and release from pipes, contaminant intrusion, nitrification, and disinfection by-products as future water quality concerns (Bernosky et al, 2005). Research has indicated the enhanced survival of pathogenic microbes in biofilms (Skraber et al, 2005; Percival & Walker, 1999). Sudden changes in flow can create aggressive shear forces, posing potential health risks to consumers by causing materials that affect water quality to be removed from pipe walls or biofilms and mobilized with the flow (Boxall et al, 2003). Although recognized intrusion events are not well-documented (Besner et al, 2011), low or negative transient pressure inside a pipe allows contaminants to enter the pipe if intrusion pathways (e.g, pipeline leaks) and contaminant sources are present. Blackburn et al (2004), Payment et al (1997), and Geldreich et al (1992) studied waterborne disease outbreaks that were possibly related to intrusion events. Suggesting intrusion as a possible mechanism of contamination for the distribution systems studied, the National Research Council (2006) highlighted low disinfectant residuals and transient pressures as potential causes of the gastrointestinal illnesses experienced by consumers of tap water.

Kirmeyer et al (2001) provided a detailed list of causes of low or negative pressure events in the daily operation of a distribution system, including valve operation, pump trip resulting from a power failure, main breaks, flushing operations, and so on. Pressure monitoring studies (Besner et al, 2011; Hooper et al, 2006; Gullick et al, 2005, 2004; Kirmeyer et al, 2001) have also indicated low or negative pressures in distribution systems.

Besner et al (2011) discussed two types of low or negative pressure events: transient events lasting from milliseconds to minutes and sustained events with durations ranging from minutes to hours. Events such as the blackout that occurred in the northeastern United States Sept. 14, 2003, as well as water main breaks and isolation of repair sites, can cause sustained events (Besner et al, 2011).

Lindley (2001) pointed to adverse pressure gradient as a condition for distribution system susceptibility to contaminant intrusion in 62.8% of US waterborne disease outbreaks during 1971–98. Although Lindley did not claim it, transient flows definitely have the potential to create adverse pressure gradients and cross connections. Studying soil and water samples collected from the vicinity of leaks and during pipe repairs, LeChevallier et al (2003) and Karim et al (2003) found a range of contaminants such as coliform bacteria, *Bacillus* species, and viruses immediately external to water distribution systems. Kirmeyer et al (2001) ranked pathogen entry routes into distribution systems and reported a high risk of intrusion via water main breaks or repairs and cross connections. The amount of leakage in water distribution systems around the world is often high (in some municipalities, leaks account for as much as 50% of the water distributed). Such systems are vulnerable to contamination because the leakage points or broken pipes can provide pathways for intrusion.

Available water quality models largely ignore the effects of inertia and compressibility and assume either steady or quasi-steady flow conditions. Certainly, steady or quasi-steady models, such as EPANET (Rossman, 2000) and its derivatives, provide an overall understanding of distribution system flows. Yet real systems undergo transient conditions in which both fluid inertia and compressibility effects are significant. Continuous variations in demand, along with the operation of devices such as valves and pumps, create events that cannot be captured by steady or quasi-steady models. A realistic model can more reliably and efficiently delineate the operating strategies that must be undertaken to ensure acceptable water quality.

Using one-dimensional (1-D) assumptions for flow and lumping together chlorine decay at the bulk and wall regions of the pipe, Fernandes and Karney (2004) studied transient hydraulic conditions and chlorine transport in a pipe. Because a 1-D model cannot capture radial variations in concentration, Naser and Karney (2008, 2007) developed and compared transient 1-D and two-dimensional (2-D) water quality models of flow inside a pipe. There were no significant differences between the models when the process of chlorine decay occurred in a bulk region, but the 2-D simulation yielded more realistic results than its 1-D counterpart when chlorine decay occurred at the pipe wall. However, the 2-D model's advantages in representing flow and water quality were severely compromised by computational requirements and simulation time. This makes a 2-D simulation computationally impractical for analyzing a real-life distribution system.

Fernandes and Karney (2004) also reported on a method of characteristics as a computationally efficient model for analyzing transient hydraulics in a distribution system. Wood et al (2005) showed that both the method of characteristics and the wave characteristic method always lead to identical results. The literature provides Eulerian, Lagrangian, and mixed Eulerian–Lagrangian models for modeling contaminant transport in pipes (Andrade et al, 2010; Basha & Malaeb, 2007; Rossman, 2000). Table 1 lists the published water quality models. The prime assumption in all the currently available Lagrangian or mixed Eulerian–Lagrangian models is that flow velocity remains unchanged (i.e., steady-state hydraulic conditions). Moreover, in comparing Eulerian and Lagrangian methods, Rossman and Boulos (1996) argued that Lagrangian methods are more computationally efficient in terms of central processing unit simulation time and memory use. They also indicated that Eulerian methods were subject to numerical dissipation (or amplitude) and dispersion (or phase shift) errors. Lagrangian methods, on the other hand, were free of numerical dissipation and dispersion errors.

The specific aim of this research was to develop a water quality model for studying contaminant intrusion and its subsequent propagation. The model was developed by coupling an Eulerian-based transient hydraulic model with a Lagrangian-based contaminant-transport model. The transient hydraulic model was required to detect junctions where negative pressure was occurring. The Lagrangian-based contaminant-transport model simulated contaminant transport along the system in a more compu-

TABLE 1 Summary of existing water quality models

Contaminant Transport Model			
Numerical Scheme	**Governing Equation**	**Hydraulic Model**	**Authors**
Lagrangian event-driven method	Advection–reaction equation	Steady-state modeling	Boulos et al, 1994
Eulerian finite-difference method Eulerian discrete-volume method Lagrangian time-driven method Lagrangian event-driven method	Advection–reaction equation	Steady-state modeling	Rossman & Boulos, 1996
Eulerian–Lagrangian method	Advection–diffusion–reaction equation	Steady-state modeling	Tzatchkov et al, 2002
Eulerian finite-difference method	Advection–reaction equation	Transient analysis	Fernandes & Karney, 2004
Lagrangian modified event–driven method	Advection–reaction equation	Steady-state modeling	Munavalli & Kumar, 2004
Eulerian–Lagrangian method	Advection–diffusion–reaction equation	Steady-state modeling	Basha & Malaeb, 2007

tationally efficient way. The proposed new model was used to simulate contaminant intrusion in two well-known water distribution systems described in the literature. Hazards and vulnerabilities of the systems were evaluated to demonstrate the applicability of the proposed model.

LAGRANGIAN–EULERIAN TRANSIENT MODEL

As shown in Figure 1, the proposed model consists of an Eulerian-based transient hydraulic model, an ingress model, and a Lagrangian-based contaminant-transport model.

Eulerian-based hydraulic model. Because most water quality models used in practice assume steady or quasi-steady flow conditions, they ignore rapid transient events and thus would not even register the negative pressure events that create the conditions required for intrusion.

In this research, hydraulic flow conditions during a transient pressure event were determined through the solutions of a hyperbolic set of partial differential equations of continuity and momentum (Boulos et al, 2005):

$$\frac{\partial H}{\partial t} + \frac{a^2}{g}\frac{\partial V}{\partial x} = 0 \quad (1)$$

$$\frac{\partial V}{\partial t} + g\frac{\partial H}{\partial x} + \frac{fV|V|}{2d} = 0 \quad (2)$$

in which H is the piezometric head, a is the acoustic wave speed (and is a function of fluid compressibility and pipe elasticity as well as pipe diameter and thickness), V is the flow velocity, t is time, g is the acceleration caused by gravity, x is the distance along the pipe's center line, f is the Darcy–Weisbach friction factor, and d is the internal pipe diameter.

A fixed-grid method of characteristics replaces Eqs 1 and 2 with an equivalent set of ordinary differential equations (Boulos et al, 2005; Larock et al, 2000). With the use of a finite difference scheme, the resulting equations were then integrated along two characteristic lines:

$$dx/dt = \pm a \quad (3)$$

With the method of characteristics solution, the time step determined by the hydraulic model (Δt) must be common to all the pipes in the system. Indeed, a common Δt forces the characteristic lines to meet at the pipe junctions. As Eq 3 suggests, the method of characteristics provides satisfactory results only if the Courant number (i.e., the ratio of wave speed over numerical speed) is 1. Moreover, Karney and Ghidaoui (1997) argued that Courant numbers less than one increase numerical dissipation. It is impossible, however, to achieve a Courant number of 1 for all the pipes in a real-life distribution system. Although an interpolation technique can be used, the wave speed or pipe length is adjusted in practice (Karney & Ghidaoui, 1997).

Typical boundary devices in a water distribution system include reservoirs, tanks, pumps, valves, and air chambers. The boundary devices were incorporated into the hydraulic model as externally imposed conditions on velocity, pressure head, or both. Chaudhry (1979) provides additional details on modeling boundary devices.

FIGURE 1 Flow chart of the Lagrangian-based transient water quality model

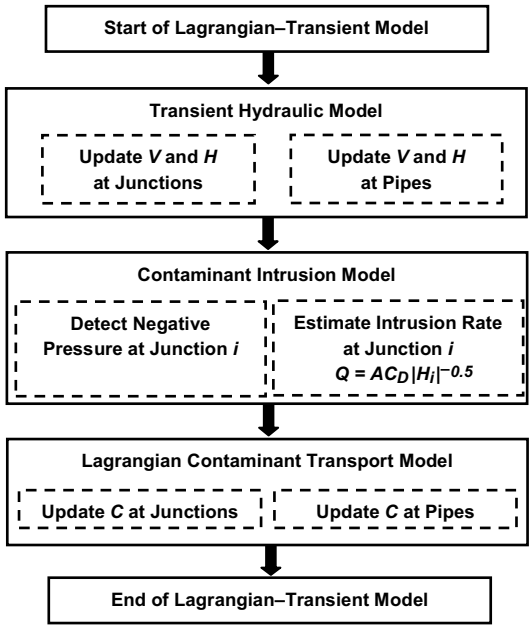

A—area of the leak point, *C*—contaminant concentration, C_D—discharge coefficient, *H*—piezometric head, *Q*—intrusion flow rate, *V*—velocity

Ingress model. An external contaminant may enter a distribution system through a leaky junction (i) when the internal pipe head (H_{int_i}) is lower than the external piezometric head (H_{ext_i}). The intrusion flow rate at a typical junction can be estimated by using either the original orifice equation (Besner et al, 2011; McInnis, 2004) or the equation proposed by Mansour-Rezaei and Naser (2013). The model of Mansour-Rezaei and Naser can provide a more realistic estimate of intrusion rates because it takes into account the characteristics of soil surrounding a pipe. However, in this research, the original orifice equation was used because of a lack of detailed information about the surrounding environment of the two distribution system cases adopted from the literature. The original orifice equation can be stated as

$$Q_i^* = C_D A\sqrt{2g\Delta H_i} \quad (4)$$

in which Q_i^* is the intrusion flow rate at the leaky junction, C_D is the dimensionless discharge coefficient, A is the area of the leak point, and ΔH_i is the difference in piezometric head across the leaky junction. Although the soil surrounding the leak point will be saturated, for the sake of simplicity, in this research the external piezometric head was assumed to be negligible. In other words, intrusion can potentially occur when internal pipe pressure head is negative.

Lagrangian-based contaminant transport model. The transport of a conservative contaminant can be modeled by an advection–diffusion equation. However, because of the high velocities in most pipes, advection is often the dominant transport mechanism (Naser & Karney, 2008, 2007). Thus, in this research diffusion was ignored, and the transport of a conservative contaminant was modeled with the following advection equation:

$$\frac{\partial C}{\partial t} + V\frac{\partial C}{\partial x} = 0 \quad (5)$$

in which C is the contaminant concentration. The contaminant was assumed to be conservative for simplicity's sake, although the model can easily be modified for a nonconservative contaminant. The research considered no changes in contaminant fate at the site of a partially or fully open valve and operating pump. A fully closed valve or a pump in off mode was modeled as a no-flux boundary.

Suppose a typical leaky junction (i) was polluted during successive hydraulic time steps when an external contaminant entered the junction or reached it through incoming flows from other pipes. With the assumption of complete and instantaneous nodal mixing, the contaminant concentration at i was calculated with the following equation:

$$C_i = \frac{\sum_{j=1}^{n} Q_j C_j + Q_i^* C_i^*}{\sum_{j=1}^{m} Q_j + Q_i^*} \quad (6)$$

in which C_i is the contaminant concentration at the leaky junction, m is the number of pipes joining the leaky junction, j is the pipe that discharges into the leaky junction, Q_j is the incoming discharge to the leaky junction, C_j is the contaminant concentration at the end of pipe j, Q_i^* is the intrusion flow rate, and C_i^* is the concentration of the intruded contaminant at the leaky junction. Although Ho (2008) confirmed that the assumption of complete mixing is sometimes inaccurate, complete and instantaneous nodal mixing is often accepted in distribution system modeling for the purpose of simplifying both simulation and data acquisition.

In this research, the contaminated water was considered as a set of discrete parcels moving along a distribution pipe, and a Lagrangian-based transport model was used to solve Eq 5. Figure 2 illustrates the steps comprising the contaminant transport model. Both the volume of a contaminant parcel (VCP) and the concentration of a contaminant parcel (CCP) were defined so the fate of a contaminant parcel along the system could be estimated.

$$VCP_k = \Delta t A_k \sum_{p=1}^{n} V_k(t_p) \quad \text{for } t_1 < t_p < t_n \quad (7)$$

$$CCP_k = \frac{\sum_{p=1}^{n} C_i(t_p)}{n} \quad (8)$$

in which VCP_k is the volume of a contaminant parcel moving along the pipe (k), Δt is the time step determined by the hydraulic model, A_k is the cross-sectional area of the pipe, n is the number of time steps during which a contaminant exists at the leaky junction, $V_k(t_p)$ is the velocity at the beginning of the pipe, t_p is a time at which the contaminant exists at the leaky junction upstream of the pipe, t_n is the last time at which the contaminant exists at the upstream junction, CCP_k is the concentration of a contaminant parcel moving along the pipe (k), and $C_i(t_p)$ is the contaminant concentration at the upstream junction calculated by Eq 6.

FIGURE 2 Lagrangian contaminant transport model

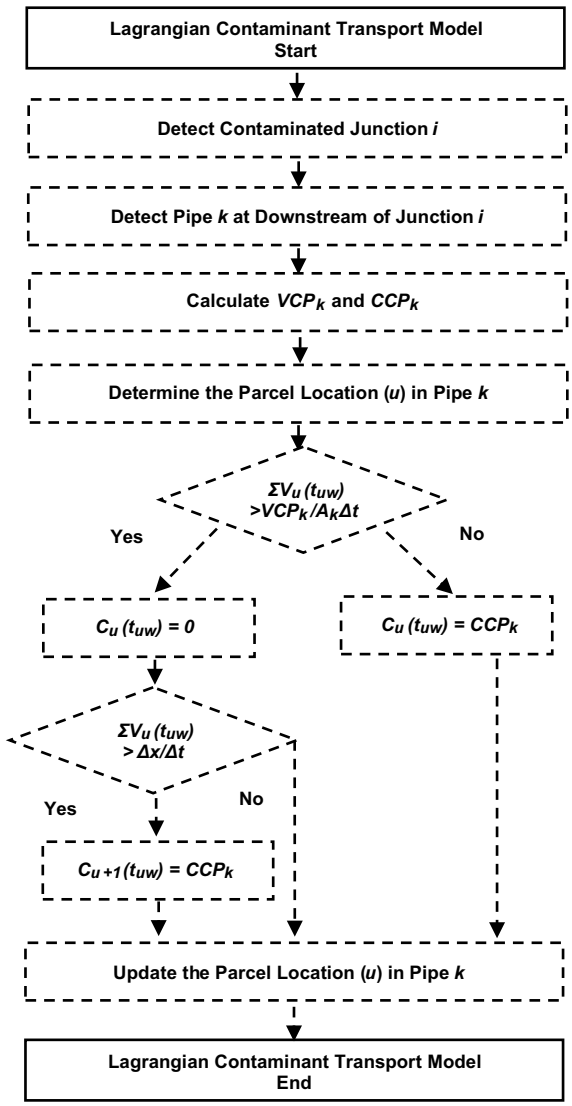

A_k—cross-sectional area of pipe k, CCP_K—concentration of a contaminant parcel moving along pipe k, C_u—contaminant concentration at internal node u, Δt—hydraulic model time step, Δx—hydraulic model space increment, t_{uw}—time equal to the w^{th} hydraulic time step after contaminant reaches internal node u, VCP_K—volume of a contaminant parcel moving along pipe k, $V_u(t_{uw})$—velocity at internal node u at time t_{uw}

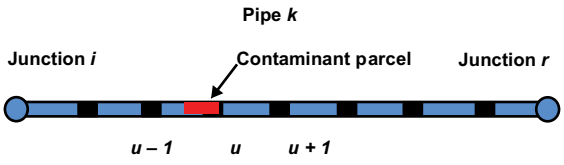

FIGURE 3 Contaminant parcel reaches node u at time t_{u1}

Junction *i*—upstream junction (circle at left end of pipe), Junction *r*—downstream junction (circle at right end of pipe)

Squares along pipe length—internal nodes

Figure 3 shows a typical pipe and its upstream and downstream junctions, i and r. The figure also indicates the internal nodes assigned by the numerical hydraulic model. When the contaminant parcel in the pipe reaches an internal node (u) at time t_{u1}, the contaminant concentration at node u changes from zero to CCP_k (assuming no dispersion, degradation, adsorption, or absorption) To determine the contaminant concentration at node u at time t_{uw}, $\Sigma V_u(t_{uw})$ was calculated, in which t_{uw} shows the time equal to the w^{th} hydraulic time step after the contaminant reaches the internal node u. When this summation exceeds $VCP_k/(A_k\Delta t)$, the contaminant parcel moves away from node u, and the concentration at node u changes from CCP_k to zero. When this summation exceeds $\Delta x/\Delta t$, the contaminant parcel reaches the node $u + 1$, and the concentration at node $u + 1$ changes from zero to CCP_k.

As time advances, the contaminant parcel reaches the junction downstream of the pipe. At this time, the contaminant parcel may be divided into new parcels, depending on the flow rates leaving the junction. As a parcel leaves the system through nodal demand at the downstream junction (r), the remaining parcels travel along the other pipes leaving this junction. With the use of Eqs 7 and 8, VCP and CCP can be calculated for the pipes receiving water from junction r. When the duration of a contaminant intrusion is relatively long, several contaminant parcels (rather than one) are introduced at the beginning of each pipe and move along each pipe's length. Then the fate of the contaminant parcels can be simulated using the proposed algorithm.

HAZARD AND VULNERABILITY INDEXES

When a contaminant intrudes into a water distribution system, hazardous and vulnerable junctions must be detected in order for the contamination threat to be managed. This research used the hazard and vulnerability indexes initially defined by Xin et al (2012). The hazard indexes for a junction were calculated by evaluating the effects of intrusion on the downstream junctions. Cumulative mass (CM) and peak concentration (PC) were the two hazard indexes used. Assuming that intrusion occurred at the upstream junction (i), the cumulative mass (CM_i) and peak concentration (PC_i) delivered to the other junctions were estimated with the following equations:

$$CM_i = \sum_{r=1}^{N, r \neq i} \sum_{t=0}^{T} C_{rt} Q_{rt} \Delta t \tag{9}$$

$$PC_i = \sum_{r=1}^{N, r \neq i} \max_{t=1 \rightarrow T} (C_{rt} Q_{rt}) \tag{10}$$

in which N is the total number of junctions, T is the response time (the period during which variations in contaminant concentration at junctions was observed), Q_{rt} and C_{rt} are demand and contaminant concentration at junction r at time t, and Δt is the time step.

The vulnerability indexes for a typical junction were calculated by evaluating the effects of intrusion on this junction when the intrusion occurred at all the other junctions. Similar to the research reported by Xin et al (2012), this research used total cumulative mass (TCM) and total peak concentration (TPC) as the vulnerability indexes, which were estimated with the following equations:

$$TCM_r = \sum_{i=1}^{N, i \neq r} \sum_{t=0}^{T} C_{ti} Q_{ti} \Delta t \tag{11}$$

$$TPC_r = \sum_{i=1}^{N, i \neq r} \max_{t=1 \rightarrow T} (C_{ti} Q_{ti}) \tag{12}$$

To allow comparison among the results, the hazard and vulnerability indexes were normalized using the minimum and maximum values calculated for a distribution system by Xin et al (2012).

$$G[\text{Index}\}_i = \frac{[\text{Index}]_i - \min_{i=1 \rightarrow N} [\text{Index}]_i}{\max_{i=1 \rightarrow N} [\text{Index}]_i - \min_{i=1 \rightarrow N} [\text{Index}]_i} \tag{13}$$

in which G_i is the normalized value of an index calculated for junction i.

RESULTS OF MODEL APPLICATIONS AND DISCUSSION

Case study 1. The proposed hydraulic and water quality model was used to examine flow conditions in the water distribution system studied initially by Boulos et al (2005) and later by Wood et al (2005) and Jung et al (2009). Figure 4 is a schematic view of the system, which consists of nine pipes, five junctions, a constant-head reservoir, and a valve. Junction numbers are inside circles, pipe numbers are inside squares, and arrows show flow directions in the pipes before the valve was closed.

Table 2 indicates the diameter, length, friction factor, and wave speed of each pipe. All junctions were at the same elevation. The reservoir head was 80 m. Demand at junctions 1–5 was 0.6 (21.2), 0.5 (17.7), 0.5 (17.7), 0.6 (21.2), and 0.5 (17.7) m^3/s (cu ft/s), respectively. Demand at the valve located at the downstream end of pipe 7 was 0.5 m^3/s (17.7 cu ft/s). Operation of the system for 50 s resulted in steady-state discharges of 3.2 (113), 1.42 (50.1), 1.28 (45.2), 0.52 (18.4), 0.41 (14.5), 0.84 (29.7), 0.5 (17.7), 0.26 (9.2), and 0.25 (8.8) m^3/s (cu ft/s) in pipes 1–9, respectively. A transient scenario was created by closure of the valve for 1 s. The valve's local-loss coefficient (K_L)

FIGURE 4 Schematic view of the distribution network in case study 1

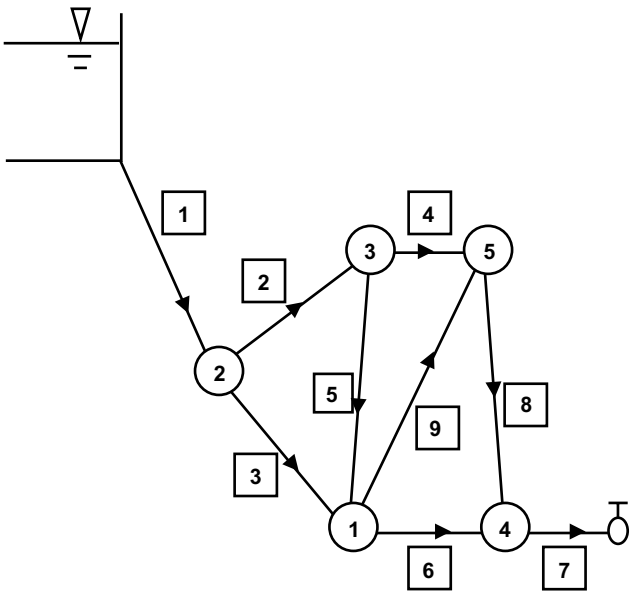

The system consists of nine pipes, five junctions, a constant-head reservoir, and a valve. Figure shows junction numbers inside circles and pipe numbers inside squares; arrows indicate flow direction.

was set as 0.19, 1.15, 5.6, and 31.9 for openings of 100, 80, 60, 40, and 20%, respectively.

To find Δt and Δx for the hydraulic model, the minimum required number of sections for the shortest pipe was defined. Then, Δx was set as the pipe length divided by the minimum number of sections for the shortest pipe. By knowing a and Δx and assuming the Courant number to be one, Δt could be calculated for the shortest pipe. The calculated Δt was considered the common (fixed) Δt for all the pipes. The number of divisions for other pipes was then calculated so that the Courant number was as close to one as possible.

Figure 5 shows the variations in piezometric head that occurred over time at junctions 1–5. As shown in the figure, the valve closure resulted in pressure drops of 41.4 to –3, 49.7 to –6.3, and 38.1 to –6.8 m at junctions 1, 3, and 4, respectively. At these junctions, the negative pressures lasted 2.2, 0.9, and 0.8 s, respectively. The distribution system reached a new steady-state hydraulic condition after ~ 100 s. The study indicated 2.07 (95.3), 1.18 (41.7), 1.02 (36), 0.38 (13.4), 0.3 (10.6), 0.54 (19.1), 0.0, 0.06 (2.1), and 0.18 (6.4) m^3/s (cu ft/s) for the new steady-state discharges at pipes 1–9, respectively.

In the presence of an intrusion pathway and a contaminant source, an external contaminant may enter the system at junctions 1, 3, and 4. For the sake of simplicity, in this research it was assumed that the pathway and contaminant source existed only in the vicinity of junction 3; therefore, intrusion occurred at this junction. With the magnitude of negative pressure taken into account, Eq 4 was used to estimate the intrusion rate at junction 3 at each time step. In Eq 4, C_DA was assumed to be equal to 0.01 m^2. Eq 6 was used to calculate the contaminant concentration at junction 3 during the intrusion, and the external contaminant concentration was assumed to be 0.03 mg/L. Figure 6 shows the variations in contaminant concentration and piezometric head at junction 3 over time. Figure 6 demonstrates two facts: intrusion occurred during the period of negative pressure, and the lower negative pressure caused more contaminant intrusion.

Because of contaminant intrusion at junction 3, two parcels of a conservative contaminant were introduced at the beginning of pipes 4 and 5 and allowed to travel with the flow along the two pipes. Eqs 7 and 8 were used to calculate the volume and concentration of the contaminant parcels as they moved along pipe 4 (VCP_4, CCP_4) and pipe 5 (VCP_5, CCP_5). VCP_4, CCP_4, VCP_5, and CCP_5 were calculated at 0.36 m^3, 4.9×10^{-4} mg/L, 0.30 m^3, and 4.9×10^{-4} mg/L, respectively. Because pipe 4 supplied more water than pipe 5, VCP_4 was greater than VCP_5. In addition, the calculation for both CCP_5 and CCP_4 represents the average contaminant concentration at junction 3 during the intrusion event (Figure 6).

Figure 7 shows the variations in contaminant concentration over time at junctions 1, 4, and 5. VCP_4 reached junction 5 at time 249.9 s and moved away from this junction at time 250.8 s. The contaminant concentration at junction 5 during this time period was 3.37×10^{-4} mg/L. Because of the contamination of junction 1, a contaminant parcel was introduced at the beginning of pipe 8, with VCP_8 as 0.34 m^3 and CCP_8 as 5.5×10^{-5} mg/L. This parcel reached junction 4 at time 2,472.8 s and moved away from this junction only a second later. The contaminant concentration at junction 4 during this time period was 3.3×10^{-5} mg/L. VCP_5 reached junction 1 at time 348.5 s and also moved away from this junction 1 s later. The contaminant concentration at

TABLE 2 Pipe characteristics for case study 1

Pipe Number	1	2	3	4	5	6	7	8	9
Diameter—*mm*	900	750	600	450	450	750	900	600	450
Length—*m*	610	914	610	457	549	671	610	457	488
Friction factor	0.02	0.02	0.02	0.02	0.02	0.02	0.02	0.02	0.02
Wave speed—*m/s*	1,000	1,000	1,000	1,000	1,000	1,000	1,000	1,000	1,000

FIGURE 5 Variations in head over time at junctions 1–5—case study 1

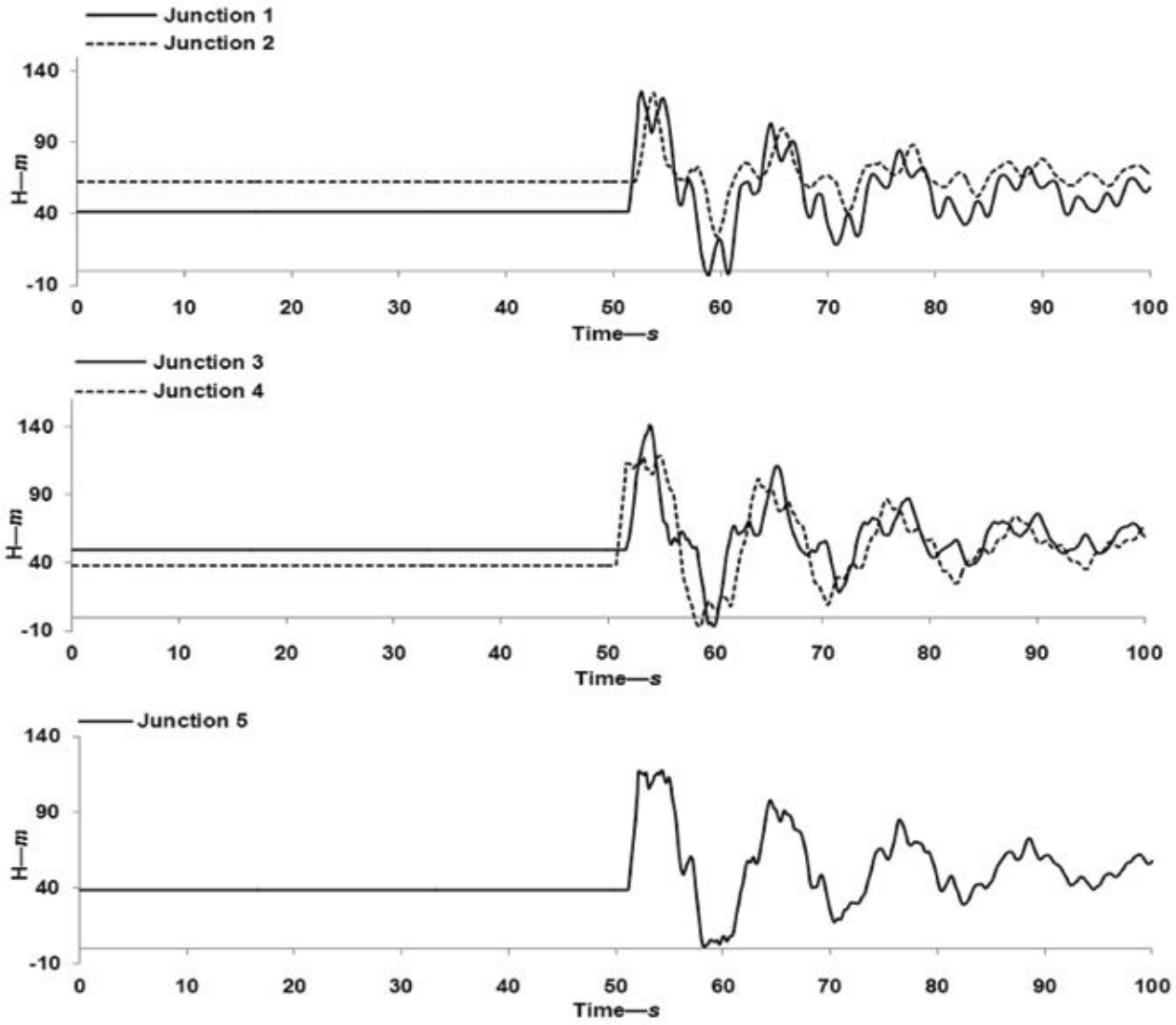

H—head

junction 1 during this time period was 1.13×10^{-4} mg/L. Because of the contamination of junction 5, two contaminant parcels were introduced at the beginning of pipes 6 and 9, with VCP_6 and VCP_9 as 0.54 and 0.18 m^3 and CCP_6 and CCP_9 as 1.13×10^{-4} mg/L. VCP_6 reached junction 4 at time 895.9 s and moved away from junction 4 at time 896.9 s. The contaminant concentration at junction 4 during this time period was 1.0×10^{-4} mg/L. VCP_9 reached junction 5 at time 786.5 s and moved away from this junction at time 787.5 s. The contaminant concentration at junction 5 during this time period was 3.6×10^{-5} mg/L. Another contaminant parcel was introduced at the beginning of pipe 8, with VCP_8 and CCP_8 equal to 0.06 m^3 and 3.6×10^{-5} mg/L, respectively. This contaminant parcel reached junction 4 at time 3,007.8 s and moved away from junction 4 at time 3,008 s. The contaminant concentration at junction 4 during this time period was 3×10^{-6} mg/L and almost certainly was associated with the brief occurrence of negative pressure.

To demonstrate the applicability of the proposed water quality model, hazard and vulnerability in this case study were evaluated by means of indexes defined by Eqs 9–13. All possible intrusion scenarios (i.e., intrusion at junctions 1, 3, and 4) were evaluated. Table 3 shows results for normalized values of the hazard and vulnerability indexes $G(CM)$, $G(PC)$, $G(TCM)$, and $G(TPC)$. Although negative pressures occurred at junction 4, the hazard indexes for this junction were zero because discharge at the downstream valve is zero after closure. The $G(CM)$ and $G(PC)$ indexes in Table 3 showed junctions 1 and 3 as the hazardous junctions in relation to contaminant

FIGURE 6 Variations in head and contaminant concentration at junction 3—case study 1

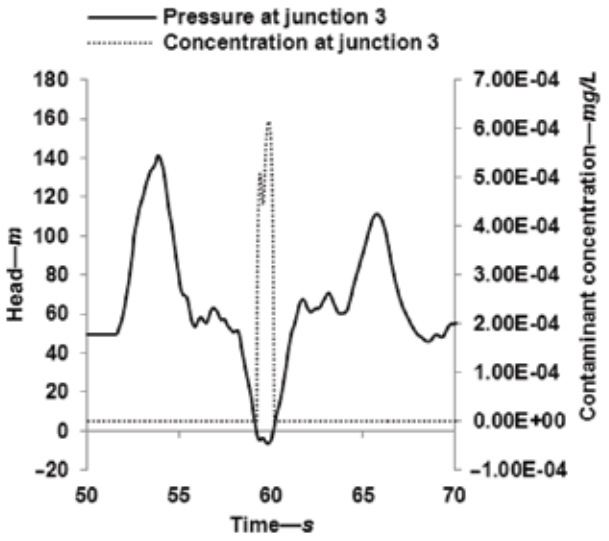

intrusion into this system. Furthermore, the cumulative mass delivered to the junctions located downstream of junction 1 was higher than the peak concentration delivered to those junctions. The magnitude of negative pressure at junction 1 (–3 m) was greater than that at junction 3 (–6.3 m). Thus, the concentration of a contaminant that intruded at junction 1 was expected to be lower than its concentration at junction 3. In addition, the flow coming to junction 1 from pipe 3 (0.54 m^3/s, or 19.1 cu ft/s) and pipe 5 (1.02 m^3/s, or 36 cu ft/s) was higher than that coming to junction 3 from pipe 2 (1.02 m^3/s, or 36 cu ft/s), causing more dilution of the intruded contaminant at junction 1. The $G(CM)$ index at junction 1 was higher than that at junction 3 because the duration of negative pressure (and thus the intrusion) at junction 1 (2.2 s) was longer than the duration at junction 3 (0.9 s).

Table 3 also shows the vulnerability indexes. Junction 5 was the most vulnerable junction in this system because it was located right after hazardous junctions 1 and 3. Junction 2 was not vulnerable because it was not affected by intrusion. Although junction 3 was a hazardous junction, it was not vulnerable to intrusion. The vulnerability of junction 1 was less than that of junction 4. Junction 1 was affected by intrusion at junction 3, and junction 4 was affected by intrusion at both junctions 1 and 3.

Case study 2. The proposed water quality model was also used to examine a water distribution system studied by Boulos et al (2005). Figure 8 is a schematic view of this system, which consists of 21 pipes, 16 junctions, a constant-head reservoir, two tanks, and a pump. Arrows indicate the flow direction before the pump was tripped.

Table 4 shows the diameter, length, friction factor, and wave speed for each pipe in the system. All junctions were located at the same elevation. The reservoir head was 70 m, and the initial

FIGURE 7 Variations in contaminant concentration at junctions 1, 4, and 6 resulting from the intrusion at junction 3—case study 1

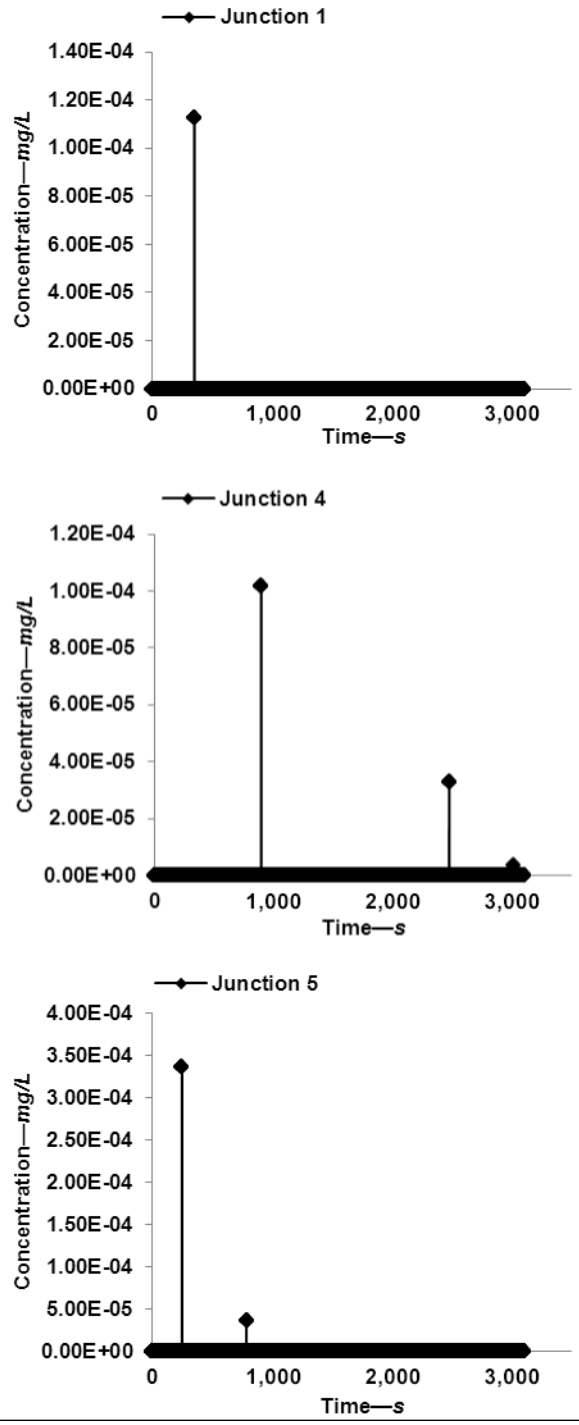

head at both tanks was also 70 m. Demand at junctions 1, 2, 5–8, 9–11, and 13 was 0.025 m^3/s (0.88 cu ft/s), whereas demand was equal to zero at junctions 3–4, 7, 12 and 14–16. After 200 s of steady-state operation, a transient scenario occurred in the network as a result of the pump failure. Table 4 also shows the steady-state discharges in the pipes before and after the pump

TABLE 3 Hazard and vulnerability evaluations for case study 1

Junction Number	Hazard Indexes		Vulnerability Indexes	
	G(CM)	*G(PC)*	*G(TCM)*	*G(TPC)*
1	1	0.23	0.31	0.37
2	0	0	0	0
3	0.19	1	0	0
4	0	0	0.93	0.58
5	0	0	1	1

CM—cumulative mass, *G*—normalized value of index, *PC*—peak concentration, *TCM*—total cumulative mass, *TPC*—total peak concentration

failure. The negative discharges showed that the flow direction reversed after the pump failure.

The proposed hydraulic model was used to simulate flow conditions in the distribution network. Figure 9 shows the variations in piezometric head that occurred over time at junctions 2, 6, 11, and 14. Negative pressures of –0.9, –1.9, –1.4, and –5.3 m lasted 4.0, 0.3, 0.7, and 0.8 s at junctions 2, 6, 11, and 14, respectively. The duration of negative pressure at junction 2 was much longer than at the other junctions.

With the assumption of the existence of an intrusion pathway and a contaminant source only in the vicinity of junction 6, two contaminant parcels were introduced at the beginning of pipes 10 and 17 and allowed to travel with the flow along the two pipes. VCP_{10}, CCP_{10}, VCP_{17}, and CCP_{17} were calculated at 0.02 m^3, 3.98×10^{-3} mg/L, 0.005 m^3, and 3.98×10^{-3} mg/L, respectively. When VCP_{10} reached junction 2, a contaminant parcel was introduced at the beginning of pipe 2, with VCP_2 as 0.01 m^3 and CCP_2 as 3.11×10^{-3} mg/L. This parcel caused contamination of junction 9. The contaminant never reached junction 3 because the discharge at pipe 11 was zero (Table 4). When VCP_{17} reached junction 11, a contaminant parcel was introduced at the beginning of pipe 16 with VCP_{16} as 0.02 m^3 and CCP_{16} as 4.5×10^{-3} mg/L. When VCP_{16} reached junction 14, two contaminant parcels were introduced and moved along pipes 20 and 19. VCP_{20}, CCP_{20}, VCP_{19}, and CCP_{19} were 0.02 m^3, 4.5×10^{-4} mg/L, 0.007 m^3, and 4.5×10^{-4} mg/L, respectively. VCP_{20} and VCP_{19} caused contamination of junctions 5 and 2. Because of the contamination

FIGURE 8 Schematic view of the distribution network in case study 2

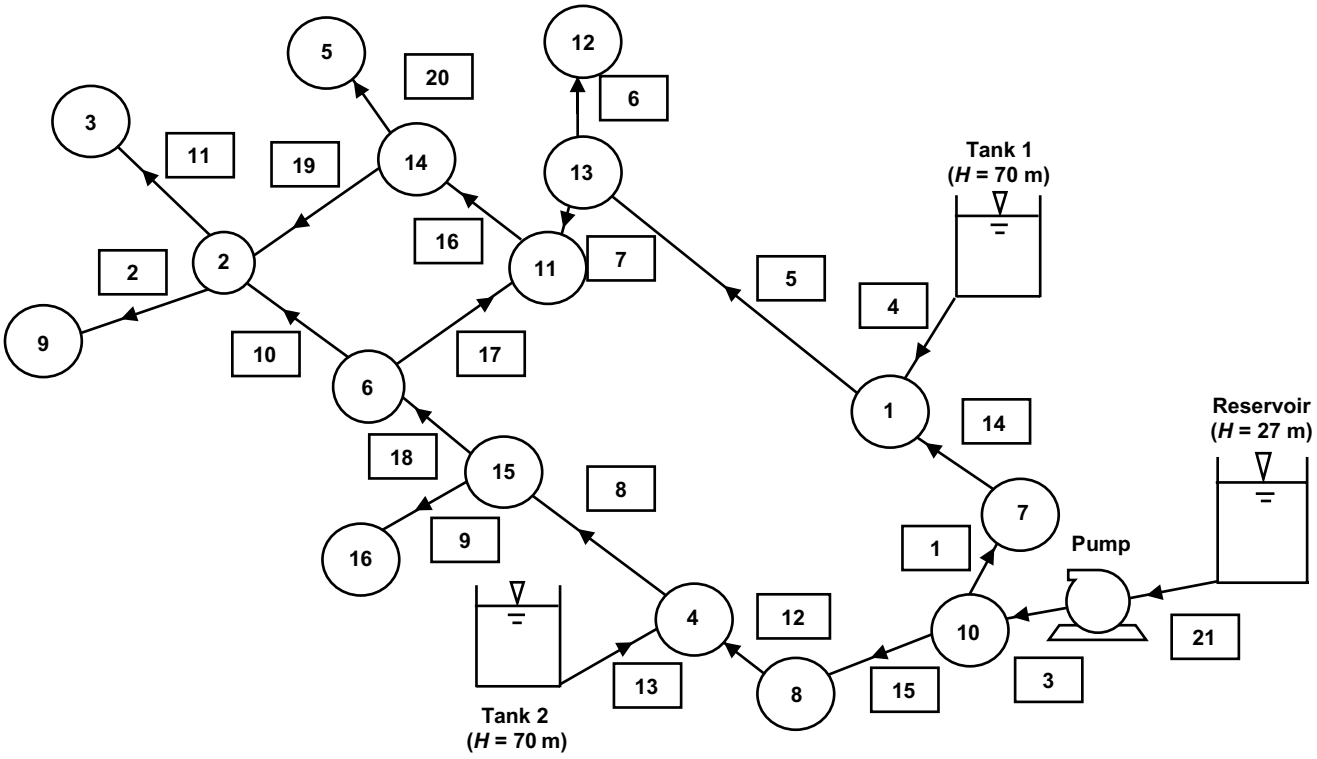

H—head

The system includes a constant-head reservoir, two tanks, and a pump. Figure shows junction numbers inside circles and pipe numbers inside squares; arrows indicate flow direction.

TABLE 4 Pipe characteristics for case study 2

Pipe Number	Diameter *mm*	Length *m*	Friction Factor	Wave Speed *m/s*	Q_1 m^3/s	Q_2 m^3/s
1	150	867	0.02	1,200	0.024	– 0.01
2	250	628	0.025	1,200	0.025	0.025
3	300	62	0.025	1,200	0.1	0
4	200	712	0.015	1,200	0.075	0.114
5	200	1,005	0.015	1,200	0.074	0.079
6	150	604	0.02	1,200	0	0
7	203	209	0.015	1,200	0.049	0.054
8	200	803	0.015	1,200	0.076	0.071
9	150	956	0.02	1,200	0	0
10	200	502	0.015	1,200	0.04	0.039
11	150	854	0.02	1,200	0	0
12	200	446	0.015	1,200	0.026	–0.04
13	200	731	0.015	1,200	0.05	0.111
14	200	777	0.015	1,200	0.024	–0.01
15	250	534	0.025	1,200	0.051	–0.015
16	200	467	0.015	1,200	0.035	0.036
17	200	896	0.015	1,200	0.011	0.007
18	200	592	0.015	1,200	0.076	0.071
19	200	1,051	0.015	1,200	0.01	0.011
20	150	387	0.02	1,200	0.025	0.025
21	300	79	0.025	1,200	0.1	0

Q_1—discharge before pump failure, Q_2—discharge after pump failure

of junction 2, the last contaminant parcel was introduced at the beginning of pipe 2, with VCP_2 as 0.02 m^3 and CCP_2 as 9.76×10^{-5} mg/L. This parcel caused contamination of junction 9. Figure 10 shows the variations in contaminant concentration over time at junctions 2, 5, 9, 11, and 14.

Vulnerability and hazard indexes were also evaluated for this case study. Table 5 shows the results for $G(CM)$, $G(PC)$, $G(TCM)$, and $G(TPC)$. Junctions 2, 6, 11, and 14 were the hazardous junctions in this distribution system. This result was expected because these were the only junctions in the system that experienced negative pressures. Junction 14 was deemed the most hazardous on the basis of both the $G(CM)$ and $G(PC)$ indexes. Hydraulic model simulations showed that junction 2 experienced the longest duration and the highest magnitude of negative pressure. Thus both the peak concentration and the cumulative mass delivered to the downstream junction were high. Although junction 2 was ranked the second most hazardous junction on the basis of the $G(CM)$ index, it was ranked the least hazardous junction on the basis of the $G(PC)$ index. The high value of $G(CM)$ at junction 2 implies that if intrusion occurred at this junction, a considerable amount of contaminant would reach the downstream junctions. Although the duration of negative pressure at junction 2 was longer than at the other junctions, the low value of $G(PC)$ shows that the concentration of contaminant reaching the downstream junctions was not high. The reason for this was the dilution at junction 2 caused by the large incoming discharge from pipe 19 (Table 4). Generally, junctions located downstream of the hazardous junctions were vulnerable.

On the basis of the $G(TCM)$ and $G(TPC)$ indexes, junctions 2, 5, 9, and 11 were considered vulnerable (Table 5). Junctions 14 and 3 were expected to be vulnerable, but because of zero demand at these junctions, the vulnerability indexes were zero. Junction 5 was deemed the most vulnerable junction on the basis of both the $G(TCM)$ and $G(TCP)$ indexes (Table 5). This was expected because junction 5 was located downstream of junction 14 (the most hazardous junction). In addition, the $G(TCM)$ index was higher than the $G(TPC)$ index for junction 9.

CONCLUSION

To study contaminant intrusion in a water distribution system, a Lagrangian-based contaminant transport model was coupled with an Eulerian-based transient hydraulic model. The hydraulic model detected negative pressures induced by events such as valve closures or pump failures. The combined water quality model was used to study contaminant intrusion in two water distribution systems described in the literature. The model derived all the benefits of Lagrangian solutions while also tracking the fate of an intruded contaminant along a distribution network. The proposed model provided a tool for evaluating the vulnerability of a water distribution system during contaminant intrusion events.

FIGURE 9 Variations in head at junctions 2, 6, 11, and 14—case study 2

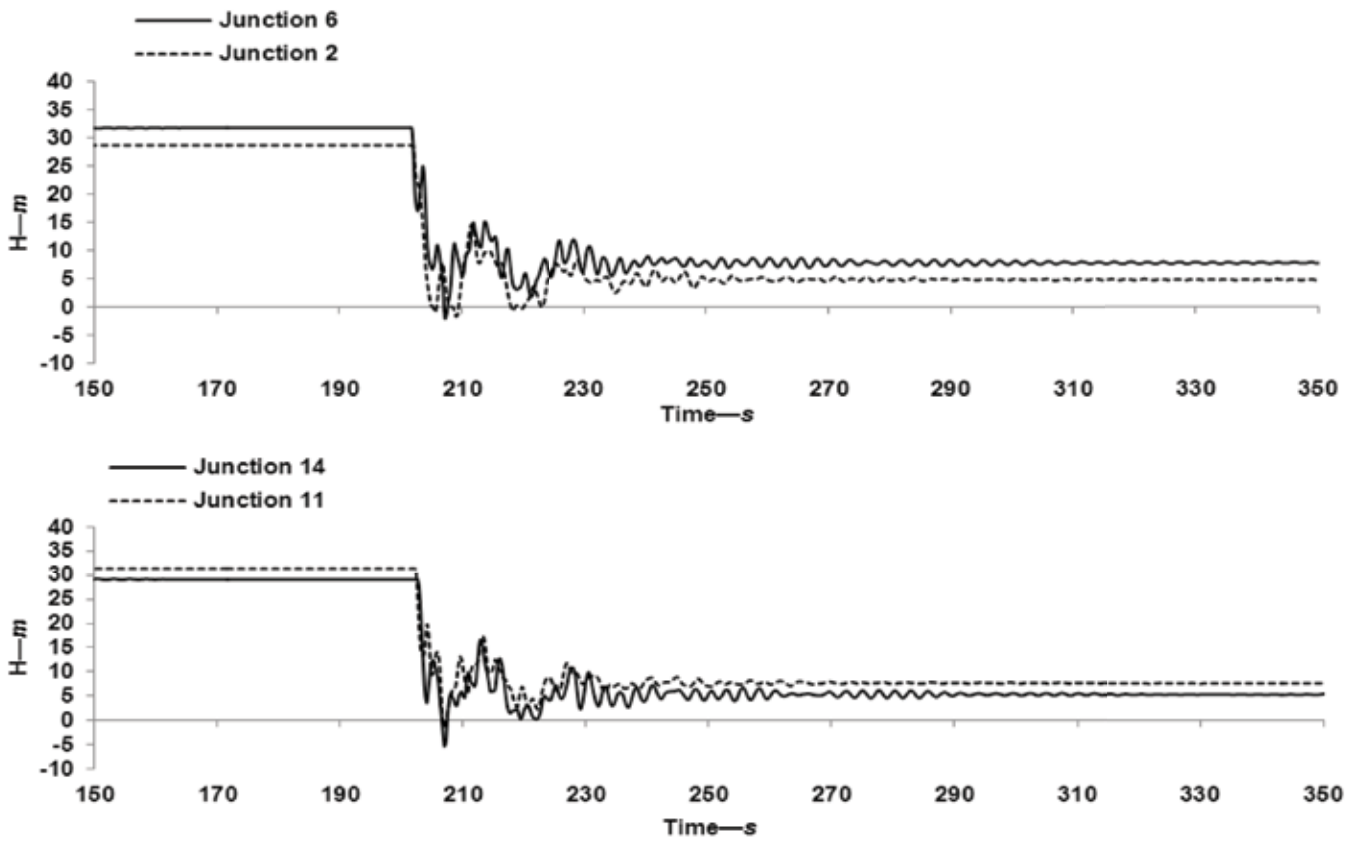

H—head

TABLE 5 Hazard and vulnerability evaluations for case study 2

Junction Number	Hazard Indexes		Vulnerability Indexes	
	G(CM)	*G(PC)*	*G(TCM)*	*G(TPC)*
1	0	0	0	0
2	0.62	0.04	0.33	0.43
3	0	0	0	0
4	0	0	0	0
5	0	0	1	1
6	0.30	0.51	0	0
7	0	0	0	0
8	0	0	0	0
9	0	0	1	0.47
10	0	0	0	0
11	0.20	0.41	0.04	0.03
12	0	0	0	0
13	0	0	0	0
14	1	1	0	0
15	0	0	0	0
16	0	0	0	0

CM—cumulative mass, *G*—normalized value of index, *PC*—peak concentration, *TCM*—total cumulative mass, *TPC*—total peak concentration

The results were then used for hazard and vulnerability evaluations of the systems.

Two practical conclusions are possible as a result of this research, though they are advanced provisionally because of the anecdotal nature of the two case studies. The first conclusion is that the contamination usually would be small and its occurrence would depend on a variety of factors conspiring to create a worst-case scenario. The second conclusion is that if contamination occurred and only scant knowledge was available about the actual system and its transient conditions, attributing any illness to the transient contaminant intrusion event would be extremely difficult.

The proposed water quality model is able to track the fate of contaminant parcels through a water distribution system. This ability is required when the duration of a contaminant intrusion is relatively long and when several contaminant parcels are introduced at the beginning of each pipe and move along the pipe lengths. However, the proposed model cannot directly track the fate of a continuous contaminant release. Also, the proposed model does not take into account mass transport caused by diffusion, dispersion, or degradation. These are important considerations, particularly in low-flow or dead-end pipes, and they can be addressed in future studies.

FIGURE 10 Variations in contaminant concentration at junctions 2, 5, 9, 11, and 14—case study 2

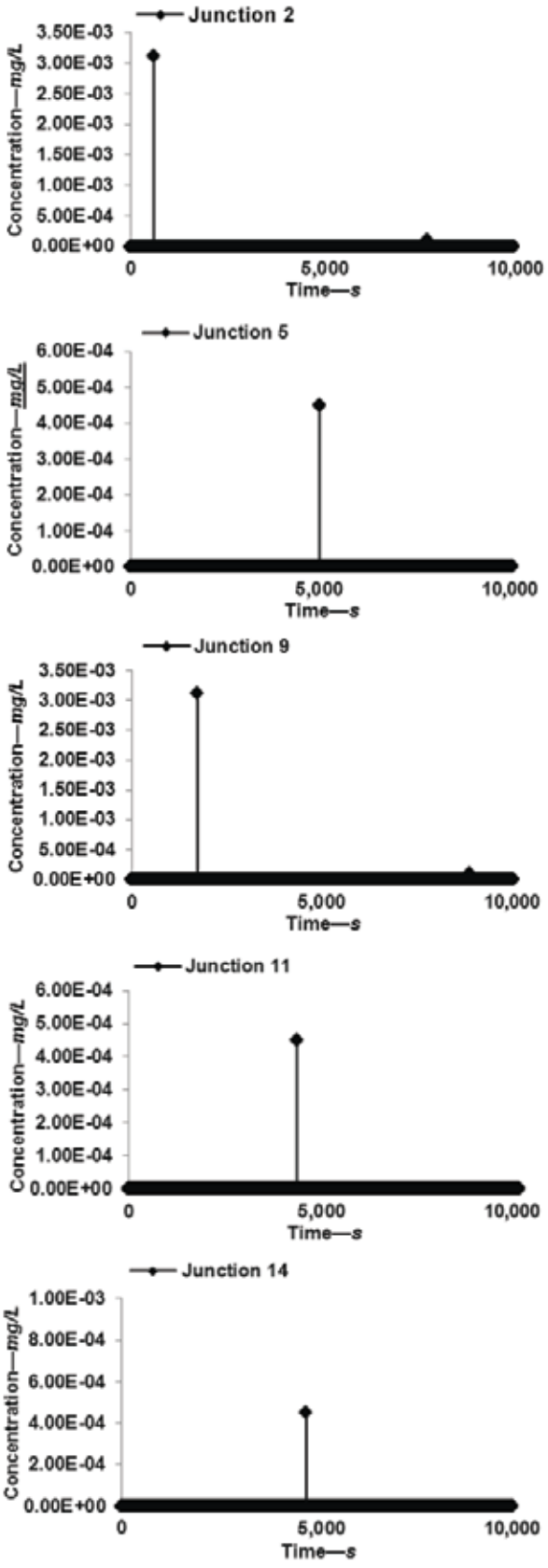

In this research, the proposed model was used when intrusion occurred at junctions; however, in real-life distribution systems, intrusion can occur wherever a leak point exists. The proposed model can be used in these cases as well, provided internal points along the pipes are defined.

ACKNOWLEDGMENT

The financial support provided by the University of British Columbia and the Okanagan Basin Water Board is greatly appreciated. The authors also thank Elodie Culiolo for technical support.

ABOUT THE AUTHORS

Saheb Mansour-Rezaei *(to whom correspondence should be addressed) is a doctoral candidate in the Okanagan School of Engineering, University of British Columbia (UBC), EME 3216-1137 University Way, Kelowna, BC V1V 1V7, Canada; sahebrezaei@gmail.com. Mansour-Rezaei has an MS degree in water resources engineering from Sharif University of Technology in Tehran, Iran, and a BS degree from the University of Tehran. Gholamreza Naser is an assistant professor in the Okanagan School of Engineering, UBC. Ahmad Malekpour is a PhD candidate and Bryan W. Karney is a professor, both in the Department of Civil Engineering, University of Toronto, Toronto, Ont.*

PEER REVIEW

Date of submission: 08/23/2012
Date of acceptance: 03/28/2013

REFERENCES

Andrade, M.A.; Rojano, F.; Romero-Gomez, P.; & Choi, C.Y., 2010. Integrated Water Quality Modeling of Water Distribution Systems. Proc. ASCE 12th Annual Conference on Water Distribution Systems Analysis, Tucson, Ariz.

Basha, H.A. & Malaeb, L.N., 2007. Eulerian–Lagrangian Method for Constituent Transport in Water Distribution Networks. *Journal of Hydraulic Engineering,* 133:10:1155. http://dx.doi.org/10.1061/(ASCE)0733-9429(2007)133:10(1155).

Bernosky, J.J.; Brown, R.A.; Cornwell, D.A.; Frey, M.M.; & Graziano, N, 2005. *Distribution System Water Quality Challenges in the 21st Century: A Strategic Guide* (M.J. MacPhee, editor). AWWA, Denver, Colo.

Besner, M-C.; Prévost, M.; & Regli, S., 2011. Assessing the Public Health Risk of Microbial Intrusion Events in Distribution Systems: Conceptual Model, Available Data, and Challenges. *Water Research,* 45:3:961. http://dx.doi.org/10.1016/j.watres.2010.10.035.

Blackburn, B.G.; Craun, G.F.; Yoder, J.S.; Hill, V.; Calderon, R.L.; Chen, N.; Lee, S.H.; Levy, D.A.; & Beach, M.J., 2004. Surveillance for Waterborne-Disease Outbreaks Associated with Drinking Water—United States, 2001–2002. *Morbidity and Mortality Weekly Report, Surveillance Summaries,* 53:8:23.

Borchardt, M.; Spencer, S.; Kieke, B.; Lambertini, E.; & Loge, F., 2009. Do Water Distribution Systems Contribute to Acute Gastrointestinal Illness Incidence? Proc. AWWA 2009 Water Quality Technology Conference, Seattle, Wash.

Boulos, P.F.; Karney, B.W.; Wood, D.J.; & Lingireddy, S., 2005. Hydraulic Transient Guidelines for Protecting Water Distribution Systems. *Journal AWWA,* 97:5:111.

Boulos, P.F.; Altman, T.; Jarrige, P-A.; & Collevati, F., 1994. An Event-Driven Method for Modelling Contaminant Propagation in Water Networks. *Applied Mathematical Modelling,* 18:2:84. http://dx.doi.org/10.1016/j.watres.2010.10.035.

Boxall, J.B.; Skipworth, P.J.; & Saul, A.J., 2003. Aggressive Flushing for Discolouration Event Mitigation in Water Distribution Networks. *Water Supply,* 3:1-2:179.

Chaudhry, M.H., 1987 (2nd ed.). *Applied Hydraulic Transients.* Van Nostrand Reinhold, New York.

Corso, P.S.; Kramer, M.H.; Blair, K.A.; Addiss, D.G.; Davis, J.P.; & Haddix, A.C., 2003. Costs of Illness in the 1993 Waterborne *Cryptosporidium* Outbreak, Milwaukee, Wisconsin. *Emerging Infectious Diseases,* 9:4:426. http://dx.doi.org/10.3201/eid0904.020417.

Environment Canada, 2001. Threats to Sources of Drinking Water and Aquatic Ecosystem Health in Canada. National Water Research Institute (Canada), Scientific Assessment Report Series, No. 1. Burlington, Ont.

Fernandes, C. & Karney, B.W., 2004. Modelling the Advection Equation Under Water Hammer Conditions. *Urban Water Journal,* 1:2:97. http://dx.doi.org/10.1080/15730620412331290038.

Geldreich, E.E.; Fox, K.R.; Goodrich, J.A.; Rice, E.W.; Clark, R.M.; & Swerdlow, D.L., 1992. Searching for a Water Supply Connection in the Cabool, Missouri, Disease Outbreak of *Escherichia coli* 0157: H7. *Water Research,* 26:8:1127. http://dx.doi.org/10.1016/0043-1354(92)90150-3.

Gullick, R.W.; LeChevallier, M.W.; Case, J.; Wood, D.J.; Funk, J. E.; & Friedman, M.J., 2005. Application of Pressure Monitoring and Modelling to Detect and Minimize Low Pressure Events in Distribution Systems. *Journal of Water Supply Research and Technology—Aqua,* 54:2:65.

Gullick, R.W.; LeChevallier, M.W.; Svindland, R.C.; & Friedman, M.J., 2004. Occurrence of Transient Low and Negative Pressures in Distribution Systems. *Journal AWWA,* 96:11:52.

Ho, C.K., 2008. Solute Mixing Models for Water-Distribution Pipe Networks. *Journal of Hydraulic Engineering,* 134:9:1236. http://dx.doi.org/10.1061/(ASCE)0733-9429(2008)134:9(1236).

Hooper, S.M.; Moe, C.L.; Uber, J.G.; & Nilsson, K.A., 2006. Assessment of Microbiological Water Quality after Low Pressure Events in a Distribution System. Proceedings ASCE 8th Annual Conference on Water Distribution Systems Analysis, Cincinnati, Ohio.

Jung, B.S.; Boulos, P.F.; Wood, D.J.; & Bros, C.M., 2009. A Lagrangian Wave Characteristic Method for Simulating Transient Water Column Separation. *Journal AWWA,* 101:6:64.

Karney, B.W. & Ghidaoui, M.S., 1997. Flexible Discretization Algorithm for Fixed-Grid MOC in Pipelines. *Journal of Hydraulic Engineering,* 123:11 1004. http://dx.doi.org/10.1061/(ASCE)0733-9429(1997)123:11(1004)

Karim, M.R.; Abbaszadegan, M.; & LeChevallier M., 2003. Potential for Pathogen Intrusion During Pressure Transients. *Journal AWWA,* 95:5:134.

Kirmeyer, G.J.; Friedman, M.; Martel, K.; Howie, D.; LeChevallier, M.; Abbaszadegan, M.; Karim, M.; Funk, J.; & Harbour, J., 2001. Pathogen Intrusion Into the Distribution System. AWWA Research Foundation, Denver, Colo.

Larock, B.E.; Jeppson, R.W.; & Watters, G.Z., 2000. *Hydraulics of Pipeline Systems.* CRC Press, Boca Raton, Fla.

LeChevallier, M.W.; Gullick, R.W.; Karim, M.R.; Friedman, M.; & Funk, J.E., 2003. The Potential for Health Risks From Intrusion of Contaminants Into the Distribution System From Pressure Transients. *Journal of Water and Health,* 1:1:3.

Lindley T.R., 2001. A Framework to Protect Water Distribution Systems Against Potential Intrusions. Master's thesis, University of Cincinnati, Cincinnati, Ohio.

Mansour-Rezaei, S. & Naser, G., 2013. Contaminant Intrusion in Water Distribution Systems: An Ingress Model. *Journal AWWA,* 105:1:37.

McInnis, D., 2004. A Relative-Risk Framework for Evaluating Transient Pathogen Intrusion in Distribution Systems. *Urban Water Journal,* 1:2:113. http://dx.doi.org/10.1080/15730620412331290010.

Munavalli, G.R. & Kumar, M.S., 2004. Modified Lagrangian Method for Modeling Water Quality in Distribution Systems. *Water Research,* 38:13: 2973. http://dx.doi.org/10.1016/j.watres.2004.04.007.

Naser, G. & Karney, B.W., 2008. A Transient 2-D Water Quality Model for Pipeline Systems. *Journal of Hydraulic Research,* 46:4:516. http://dx.doi.org/10.3826/jhr.2008.3015.

Naser, G. & Karney, B.W., 2007. A 2-D Transient Multicomponent Simulation Model: Application to Pipe Wall Corrosion. *Journal of Hydro-Environment Research,* 1:1:56. http://dx.doi.org/10.1016/j.jher.2007.04.004.

NRC (US National Research Council), 2006. *Drinking Water Distribution Systems: Assessing and Reducing Risks.* The National Academies Press, Washington, D.C.

NRCC (National Research Council Canada), 2004. Monitoring Water Quality in the Distribution System. National Guide to Sustainable Municipal Infrastructure, Version 1.0. Federation of Canadian Municipalities and NRC Canada, Ottawa, Ont.

Payment, P.; Siemiatycki, J.; Richardson, L.; Renaud, G.; Franco, E.; & Prévost, M., 1997. A Prospective Epidemiological Study of Gastrointestinal Health Effects Due to the Consumption of Drinking Water. *International Journal of Environmental Health Research,* 7:1:5. http://dx.doi.org/10.1080/09603129773977.

Percival, S.L. & Walker, J.T., 1999. Potable Water and Biofilms: A Review of the Public Health Implications. Biofouling: *The Journal of Bioadhesion and Biofilm Research,* 14:2: 99. http://dx.doi.org/10.1080/08927019909378402.

Rossman, L.A., 2000. EPANET-2 Users Manual. National Risk Management Research Laboratory, Office of Research and Development, US Environmental Protection Agency, Cincinnati, Ohio. http://dx.doi.org/10.1061/(ASCE)0733-9496(1996)122:2(137).

Rossman, L.A. & Boulos, P.F., 1996. Numerical Methods for Modeling Water Quality in Distribution Systems: A Comparison. *Journal of Water Resources Planning and Management,* 122:2:137.

Schuster, C.J.; Ellis, A.G.; Robertson, W.J.; Charron, D.F.; Aramini, J.J.; Marshall, B.J.; & Medeiros, D.T., 2005. Infectious Disease Outbreaks Related to Drinking Water in Canada, 1974–2001. *Canadian Journal of Public Health,* 96:4:254.

Skraber, S.; Schijven, J.; Gantzer, C.; & de Roda Husman, A.M., 2005. Pathogenic Viruses in Drinking-Water Biofilms: A Public Health Risk? *Biofilms,* 2:2:105. http://dx.doi.org/10.1017/S1479050505001833.

Tzatchkov, V.G.; Aldama, A.A.; & Arreguin, F.I., 2002. Advection-Dispersion-Reaction Modeling in Water Distribution Networks. *Journal of Water Resources Planning and Management,* 128:5:334. http://dx.doi.org/10.1061/(ASCE)0733-9496(2002)128:5(334).

Wood, D.J.; Lingireddy, S.; Boulos, P.F.; Karney, B.W.; & McPherson, D.L., 2005. Numerical Methods for Modeling Transient Flow. *Journal AWWA,* 97:7:104.

Xin, K.; Tao, T.; Wang, Y.; & Liu, S., 2012. Hazard and Vulnerability Evaluation of Water Distribution System in Cases of Contamination Intrusion Accidents. *Frontiers of Environmental Science & Engineering,* 6:6:839.